Appearance of supernumeraries of the secondary rainbow in rain showers

G. P. Können

Royal Netherlands Meteorological Institute, P.O. Box 201, NL-3730 AE De Bilt, The Netherlands

Received June 11, 1986; accepted January 7, 1987

The secondary rainbow scattering angle for spheroidal drops of water is virtually independent of aspect ratio for most visible wavelengths. For most solar heights the residual aspect-ratio dependence shifts the bow toward a smaller deviation angle if the drop size increases. These two facts explain why the supernumeraries of the secondary rainbow are never seen in rain showers. At high solar elevations the flattening of drops results in a shift of the secondary rainbow toward a larger deviation angle. It is shown that this shift is still large enough to cause the formation of the first supernumerary in red light. This red supernumerary of the secondary rainbow may be observable by eye in natural showers if a red filter is used to remove the obscuring contribution of shorter wavelengths to the light of the rainbow. For indices of refraction far from that of water, a strong aspect-ratio dependence of the secondary rainbow angle is shown to be present. Some possible implications of this for the formation of a hyperbolic umbilic diffraction catastrophe in the secondary rainbow pattern are indicated.

1. INTRODUCTION

A few years ago Fraser[1] offered an explanation for the paradoxial fact that supernumeraries of the primary rainbow are regularly visible in rain showers, although the broad droplet-size distribution in the showers should prevent this. The argument is the following. If the drop size is below a certain value, the shape of a falling drop remains close to spherical, and the deviation angle (which equals the scattering angle for the primary bow) of the Descartes geometrical rainbow ray is fixed. A decrease in drop size causes a wider spacing between the interference maxima in the scattering pattern of the rainbow because of the decreasing difference in optical path length between the interfering light rays in the drop. Consequently the deviation angle of a given interference maximum increases in the small-drop-size limit. Large falling drops, on the other hand, have a flattened shape, becoming more and more pronounced if the drop size increases. This oblateness causes a shift of the rainbow angle and hence of the whole rainbow scattering pattern toward a larger deviation angle for any solar elevation at which the bow is above the horizon. Therefore, the deviation angle of a rainbow interference maximum increases in both the small-size and large-size limits; for a drop radius of about 0.25 mm it has a stationary point. Owing to the existence of this stationary point, the rainbow intensity integrated over a broad drop-size spectrum still shows oscillations as a function of scattering angle; thus supernumeraries may be visible. However, the angular spacing between them contains hardly any information about the drop sizes in the shower: if the drop-size distribution is broad enough, the separation between the first and second supernumeraries is fixed at about 0.7°.

While supernumeraries of the primary rainbow are frequently observed in the open, supernumeraries of the secondary rainbow are extremely rare.[2] In this paper we describe an attempt to explain this by arguments similar to Fraser's. For this, Möbius's theory[3,4] of the Descartes rainbow angle for spheroidal drops was extended to the secondary rainbow. Contrary to what one might expect intuitively,[5] the secondary rainbow angle at visible wavelengths shows little dependence on the oblateness of the drops. The reason is that, because of the value of the index of refraction of water, the places where the secondary rainbow ray hits the wall of the water drop are about 90° from one another, as seen from the center of the drop. Therefore, the changes in direction of the Descartes ray that arise at the entrance and at the first internal reflection due to the flattening of drops are almost entirely compensated for by the changes at the next internal reflection and at emergence (see Fig. 1). This causes the aspect-ratio dependence of the secondary rainbow angle to be 1 order of magnitude smaller than in case of the primary bow.

For most solar elevations, this residual aspect-ratio dependence shifts the secondary rainbow toward a smaller deviation angle if the drop size increases (note that for the secondary rainbow the deviation angle equals the scattering angle only if the interval of the latter is taken to be [180°, 360°]). On the other hand, as in case of the primary bow, the deviation angle of an interference maximum of the secondary rainbow increases in the small-drop-size limit. Hence the deviation angle of an interference maximum as a function of drop size now lacks a stationary point. This excludes the formation of supernumeraries of the secondary rainbow in showers according to Fraser's mechanism and may explain why they are so exceedingly rare.

However, for high solar elevations (say, >35°) the flattening of drops shifts the rainbow angle into the other direction. In spite of the fact that this shift is small, it seems to be large enough to cause the formation of the first supernumerary of the secondary rainbow in showers. As the sensibility of the secondary rainbow angle to aspect ratio increases appreciably with wavelength, the conditions for supernumerary formation are substantially better for red light than for blue light. A red supernumerary of the secondary rainbow may

0740-3232/87/050810-07$02.00

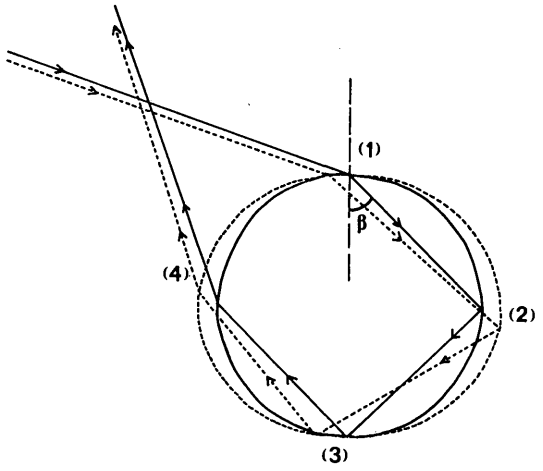

Fig. 1. Path of the ray of minimum deviation for the secondary rainbow. For a spherical drop (solid lines), the angle of refraction β of the Descartes ray is very close to 45°. Therefore, seen from the center of the drop, the difference in position angle of two subsequent hits at the wall is about 90°. If the drop becomes spheroidal (dashed lines), the path of the Descartes ray changes. However, because of this difference of 90° in position angle, the changes in light path at hits (1) and (2) are almost entirely compensated for by the subsequent changes at hits (3) and (4), so that the aspect-ratio dependence of the direction of the emerging ray remains very small. This explains why supernumeraries of the secondary rainbow in showers are extremely rare.

become visible in nature if a monochromatic filter is used to remove the obscuring background caused by rainbow scattering at shorter wavelengths.

2. RAINBOW ANGLES FOR FLATTENED DROPS

A falling drop can be approximated by an oblate spheroid, with its two semimajor axes of length a horizontal and its semiminor axis of length b vertical. This spheroid approximation holds almost perfectly for equivalent drop radii r [$\equiv(a^2b)^{1/3}$] below 0.5 mm.[6,7] For larger radii, the drop gradually develops some asymmetry. However, for r smaller than 1.2 mm, which is the case of interest here, this asymmetry is small enough to be neglected. The vertical cross section of a spheroidal drop is an ellipse with semimajor axes a and b. The ellipticity ρ, defined by Möbius, is

$$\rho = (a - b)/(a + b). \tag{1}$$

For drops falling at terminal velocity, Green[8] derived a simple relation between b/a and r. This function is given in his paper as Eq. (9). We substitute it into Eq. (1) and linearize the result by expanding in a Taylor series, which leads to

$$\rho \simeq 0.050 r^2 \tag{2}$$

if r is expressed in millimeters. This formula has an accuracy of 15% at $r = 1$ mm and is still useful up to $r = 1.5$ mm.

According to Möbius,[3,4] the geometrical primary rainbow scattering angle θ_r for spheroidal drops (in degrees) for the top of the rainbow can be found from the relation

$$\Delta\theta_r \equiv \theta_r(\text{spheroid}) - \theta_r(\text{sphere}) = \frac{180°}{\pi} 16\rho \sin\beta \cos^3\beta \cos(2h - 42°), \tag{3}$$

in which β is the angle of refraction of the Descartes ray for spheres, h is the solar elevation, and the numerical value of 42° in the last cosine is $180° - \theta_r(\text{sphere})$, the angular distance of the bow to the antisolar point. We note that an earlier discussion of the effect of the oblateness of drops on the visibility of supernumeraries[5] applied formula (3) with a plus rather than a minus in the argument of the last cosine, a result of an incorrect interpretation of Möbius's angle ψ. Therefore the final conclusions of that analysis are not valid.

Formula (3) is almost independent of wavelength. The reason is that the rainbow refraction angle $\beta \simeq 40°$ varies only by 1° in the visible range. The resulting variation in formula (3) amounts to only 2% and can therefore be neglected.

In this paper we concentrate mainly on the top of the bow and on its base if the solar elevation is low. For another scattering azimuth ζ, one can derive the analog of formula (3) by considering the ellipse resulting from the cross section of the nonvertical scattering plane with the spheroidal drop. In general, the light ray inside the drop will not be confined to the plane of this ellipse. However, for the small values of ρ considered here, deviations of the ray from that plane can be neglected, so the Möbius formula can be applied. Then one finds that for a nonvertical scattering plane one has to replace ρ by ρ' and h by h' in formula (3) or in the corresponding formula for the secondary bow [Eq. (6) below], where

$$\rho' = \rho(1 - \sin^2\zeta \cos^2 h), \qquad \tan h' = \tan h/\cos\zeta. \tag{4}$$

Here, $\zeta = 0°$ for the rainbow top and 180° for its bottom.

Formula (3) is consistent with Fraser's numerical result that $\Delta\theta_r$ is a strong function of equivalent drop radius r but only a weak function of solar elevation h for $h < 42°$. Substituting Eq. (2) into Eq. (3), we have for the top of the rainbow in visible light

$$\Delta\theta_r = 13° r^2 \cos(2h - 42°) \equiv Cr^2. \tag{5}$$

For the solar elevation range at which the rainbow is above the horizon, C is between 10° and 13°. Of course, for the rainbow base at $h = 0$, $\Delta\theta_r$ and C are zero, since the horizontal cross section of a flattened drop is a circle [see Eqs. (4)].

For the discussion of the *secondary* rainbow, it is convenient to change the interval of the scattering angle θ into [180°, 360°]. Then the scattering angle equals the deviation angle, and the secondary rainbow angle θ_r is about 231°. This procedure has the advantage that the oscillating part of the secondary rainbow occurs for $\theta > \theta_r$, just as in the case of the primary bow. This makes the description of the intensity distribution in terms of an Airy function uniform for the two rainbows, as the signs of argument in it are then equal (see Section 4).

By making arguments similar to Möbius's, one finds straightforwardly that for the top of the secondary rainbow

$$\Delta\theta_r = -\frac{180°}{\pi} 64\rho \sin\beta \cos^3\beta \cos 2\beta \cos(2h - 51°). \tag{6}$$

As before, the 51° in the last cosine is the distance of the bow to the antisolar point, which is $\theta_r(\text{sphere}) - 180°$ in this case. From Eq. (6) it is clear that $\Delta\theta_r$ is zero for $\beta = 45°$. This happens for an index of refraction $n = \sqrt{9/5} = 1.342$, because

from simple geometrical rainbow theory it follows that for the secondary rainbow

$$\cos 2\beta = \frac{5n^2 - 9}{4n^2}. \tag{7}$$

The value of $n = 1.342$ occurs for water at a wavelength of 410 nm, which is violet light.

As β varies again by only 1° in the visible range, the absolute value of $\Delta\theta_r$ is rather small, even at the red end of the spectrum. But as $\cos 2\beta$ starts from zero at violet, now a strong wavelength dependence is present in this small $\Delta\theta_r$. To calculate this, we determine from Eq. (7) the difference $\delta\beta$ between β and 45° as a function of the index of refraction, which is given to first order by

$$\delta\beta \equiv \beta - 45° = \frac{180°}{\pi}\frac{5}{4\sqrt{9/5}}(\sqrt{9/5} - n). \tag{8}$$

To derive the analog of Eq. (5) from Eq. (6), it is convenient to define

$$C_0 = \frac{32}{20}\delta\beta = 86°(1.342 - n). \tag{9}$$

For wavelengths of 410, 470, 540, 650, and 850 nm, the parameter C_0 = 0°, 0.3°, 0.6°, 0.9°, and 1.2°, respectively. Linearizing Eq. (6) near β = 45° and combining the result with Eqs. (2) and (8), one has with Eq. (9) for the secondary rainbow top

$$\Delta\theta_r = C_0 r^2 \cos(2h - 51°) \equiv C_1 r^2. \tag{10}$$

The absolute accuracy of Eqs. (3) and (6) is comparable. But since the value of $\Delta\theta_r$ for the secondary rainbow is much smaller than that for the primary bow, the linear Möbius term [Eq. (6)] alone is not able to describe the rainbow shift satisfactorily, and we also have to consider the next term, which is proportional to ρ^2. In the general form, this is a long and complicated expression, but if β is close to 45° it simplifies significantly. Expressing its wavelength dependence in C_0, we find that

$$\Delta\theta_r(\text{second order}) = \frac{180°}{\pi}\rho^2\left[-\frac{32}{3}\cos^2(2h - 51°) + 16\sin(4h - 102°)\right] - 20C_0\rho^2\left[10 + 5\sin(4h - 102°) - \frac{28}{3}\cos^2(2h - 51°)\right]. \tag{11}$$

Combining this with Eqs. (2) and (10), the ultimate result becomes

$$\Delta\theta_r = C_1 r^2 + C_2 r^4, \tag{12}$$

with

$$C_1 = C_0\cos(2h - 51°),$$
$$C_2 = -1.56°\cos^2(2h - 51°) + 2.34°\sin(4h - 102°) - C_0[\tfrac{1}{2} + \tfrac{1}{4}\sin(4h - 102°) - 7/15\cos^2(2h - 51°)]. \tag{13}$$

At low h, C_2 is of the order of −3°. It changes sign at about h = 35° and reaches a maximum value of about +1.5° near h = 52°. In the latter case the rainbow top for blue light is just at the horizon. The wavelength-dependent term in Eqs. (13), which is proportional to C_0, causes a correction of at most 0.5° in the visible range. To test Eq. (12), Fraser kindly ran his program[1] for the secondary rainbow. At r = 1.2 mm, his results compare within 20% with mine (his values being the smallest of the two), and for smaller r this difference rapidly becomes smaller.

The aim of the present study is not primarily to describe the rainbow shift $\Delta\theta_r$ itself but to investigate its effect on the rainbow intensity distribution in a broad droplet-size distribution (see Section 5). This is determined mainly by the behavior of Eq. (12) near the stationary point in the argument of the rainbow intensity distribution for individual drops [Eq. (15) below]. From Section 4, Eqs. (15), (16), *et seq.*, it follows that the stationary behavior for the secondary rainbow near its first supernumerary occurs if $r = r_s \simeq 0.7$ mm; if the complete expression for the rainbow shift, Eq. (12), is applied in the rainbow distribution, the numerical value for r_s remains about the same. Now, for our purpose we simplify Eq. (12) by putting $r^4 \simeq r_s^2 r^2 \simeq 0.5r^2$ in its second term, so that the result becomes

$$\Delta\theta_r = Cr^2,$$

with

$$C = C_1 + 0.5C_2. \tag{14}$$

Here, C is a strong function of wavelength and solar elevation. From Eqs. (13) it can be seen that the wavelength dependence is caused mainly by C_1 and the solar-elevation dependence mainly by C_2. Calculations show that the switch from Eqs. (12) to (14) is indeed permitted, as the two equations generate almost identical rainbow intensity distributions in broad droplet-size distributions such as the one used in Section 5.

3. RAINBOW INTENSITY DISTRIBUTIONS FOR SPHEROIDS

If the Airy distribution is used for the rainbow scattering function for an individual spherical drop, the corresponding intensity distribution for a spheroid with low ellipticity ρ can be found[9] simply by replacing θ_r(sphere) in the former intensity distribution by θ_r(spheroid). This can be done by using Eqs. (5) and (12) for the primary and secondary bows, respectively. So, for low ellipticities, the effect of increasing ellipticity is just a shift of the whole interference pattern, leaving the analytical form of the intensity distribution intact. This seems to hold[10] at least up to ρ = 0.1 and hence for falling drops with radii[6] up to 1.8 mm. For still larger ellipticities, the situation changes. As pointed out recently by Marston and Trinh,[10] the Airy distribution may be transformed into a hyperbolic umbilic diffraction catastrophe because two additional rays with skew paths through the oblate drops can also contribute to the rainbow interference pattern. This transformation has been observed by these authors for the primary rainbow when the scattering plane was about horizontal.

As to the secondary rainbow, at first sight one might expect a similar transformation to occur with increasing ellipticity. However, this need not be so if the strength of this out-of-plane scattering effect is closely related to the in-

plane change of the light paths and hence to the sensitivity of the rainbow angle to ellipticity. If this conjecture holds, our present findings mean that such a transformation will be absent in the case of secondary rainbow scattering by drops of water. For other liquids, such an effect may still occur, provided that the index of refraction is far enough from 1.342. The strength of the in-plane deviation of the rays of the secondary rainbow in a certain liquid becomes comparable with that of the primary rainbow in water if $|C_1| \simeq 13°$ [Eqs. (5) and (10)] and hence if $|C_0| \simeq 13°$ [Eqs. (9) and (10)]. This would happen for substances with $n \simeq 1.2$ (e.g., a drop with $n = 1.6$ suspended in water) and $n \simeq 1.5$ (e.g., benzene). In the former case $C_0 > 0$, so that the analog of the effect observed by Marston and Trinh would occur near the horizontal scattering plane again; but in the latter case $C_0 < 0$, and the effect is rather to be expected in the vertical scattering plane.

If we consider a broad drop-size distribution rather than an individual drop, the effect observed by Marston and Trinh can be neglected. The reason is that the amount of light scattered by drops with $r > 1.5$ mm is only a small fraction of the total. For instance, for the Marshall–Palmer distribution, which we will use below, a short calculation shows that this fraction is less than 1%. Therefore, in the following discussion of supernumeraries in showers we omit the effects of large drops and use the Airy approximation for the rainbow intensity distributions.

4. SPACING BETWEEN SUPERNUMERARIES IN SHOWERS

Using the Airy approximation[11] for the normalized intensity distribution of the rainbow as a function of scattering angle θ, denoting the Airy function by Ai, and describing the effect of the ellipticity by inserting Eq. (14) into it, one has for the intensity I per unit of solid angle of the secondary rainbow near θ_r ($\simeq 231°$) the following expression[12]:

$$I(r, \theta) \propto r^{7/3}\,\mathrm{Ai}^2\left\{-3.1\left(\frac{500}{\lambda}\right)^{2/3} r^{2/3}[\theta - \theta_r(\text{sphere}) - Cr^2]\right\}$$
$$\equiv r^{7/3}\,\mathrm{Ai}^2[f(r, \theta)]. \tag{15}$$

Here, r is expressed in millimeters, θ in degrees, and the wavelength λ in nanometers. For the primary rainbow ($\theta_r \simeq 138°$), Formula (15) is valid too, but then the constant 3.1 in it is replaced by 5.6, and Eq. (5) instead of Eq. (14) is used for the calculation of C.

The argument of the Airy function $f(r, \theta)$ in Eq. (15) is stationary in r at $r = r_s$; one easily confirms that the value of r_s is found by the relation

$$4Cr_s^{\,2} = \theta - \theta_r(\text{sphere}). \tag{16}$$

If $C > 0$, this stationary behavior of $f(r, \theta)$ is in the oscillating part of Ai^2. This implies that for $C > 0$, the integral of Eq. (15) over a broad drop-size distribution $Int(\theta)$ is also oscillating. This integral is the sum of a nonoscillating part and an oscillating part. The scattering angles of the maxima and minima of the oscillating part of Int are in first approximation found by substituting $r = r_s$ into $I(r, \theta)$.[13] So the spacing between two subsequent maxima in the rainbow intensity distribution Int in showers can be found by evaluating the function $\mathrm{Ai}^2[f(r_s, \theta)]$. In this way, one finds for $C = 1°$ and $\lambda = 640$ nm that the angular spacing $\theta_{1,2}$ between the first and second supernumeraries [$f(r_s, \theta) = -3.25$ and -4.82, respectively] is 0.71° for the secondary rainbow. Substituting Eq. (16) into $f(r_s, \theta)$, one finds easily that $\theta_{1,2}(\lambda, h)$ is given by

$$\theta_{1,2}(\lambda, h) = 0.71°\,C^{1/4}(\lambda, h)\left(\frac{\lambda}{640}\right)^{1/2}. \tag{17}$$

For the primary rainbow with $C = 13°$, $\theta_{1,2} = 0.88°$ at $\lambda = 640$ nm. For other wavelengths and C, a relation similar to Eq. (17) is valid. The numerical values of $\theta_{1,2}$ found in this way are consistent with Fraser's observations of the spacing between supernumeraries of the primary rainbow.[1]

5. VISIBILITY OF SECONDARY RAINBOW SUPERNUMERARIES IN SHOWERS

Formation of supernumeraries according to Fraser's mechanism requires that the factor C in Eq. (15), determining the aspect-ratio dependence of the rainbow angle, be positive. If the solar elevation is higher than 35°, this is the case for the secondary rainbow in the whole visible spectrum, as can be inferred from Eqs. (13) and (14). But even then it is by no means obvious that perceptible supernumeraries will indeed show up in showers, as the maximum value of C is 1 order of magnitude smaller than in the case of the primary rainbow.

To simulate the intensity distribution of a natural secondary rainbow, we assume that the drop-size distribution in a shower is a Marshall–Palmer distribution of the typical form[7]

$$dN/dr \propto \exp(-6r). \tag{18}$$

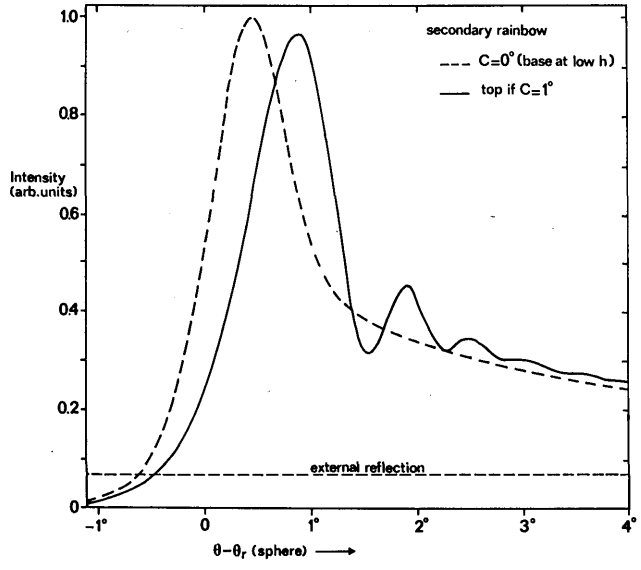

Fig. 2. Intensity of the secondary rainbow as a function of scattering angle θ, integrated over a Marshall–Palmer drop-size distribution and over the solar disk. The curve for $C = 0°$ is valid for the rainbow base if the solar elevation h is low and for its top if $h \simeq 30°$; $C = 1°$ can be realized at the rainbow top if the solar elevation is 40° or more. For the definition of C, see Eq. (14). The interval of θ has been extended over 180°, so that the scattering angle equals the deviation angle. The Descartes secondary rainbow angle for spheres, denoted by θ_r(sphere), is about 231°. The intensity of the light caused by external reflection at the drops is also indicated.

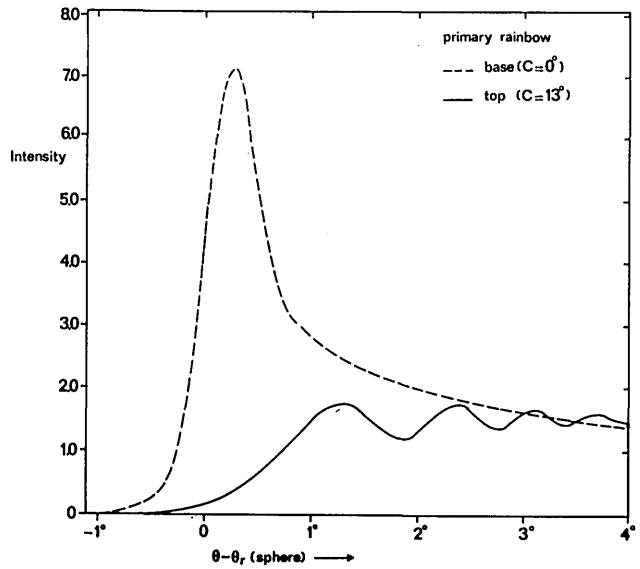

Fig. 3. Intensity of the primary rainbow as a function of scattering angle θ near the base of the bow at low solar elevation and at its top, integrated over the same drop-size distribution as the one applied in Fig. 2 and over the solar disk. Same intensity units as for Fig. 2. C is defined by Eq. (5). The Descartes primary rainbow angle for spheres, denoted by θ_r(sphere), is about 138°.

Here N denotes the number of particles and r is in millimeters. We multiplied Eq. (15) by relation (18) and integrated the result over r and over the solar disk.

Figure 2 displays the integrated secondary rainbow intensity distribution for $C = 0°$ and $C = 1°$. The former value of C is not only valid for the rainbow base at $h = 0$ but can also be realized at its top if the solar elevation is of the order of 30° [see Eqs. (13) and (14)]. If C is negative, the integrated intensity distribution is virtually identical to the one for $C = 0°$. In the figure, the intensity of light resulting from externally reflected light at the drops is depicted also. It is calculated by adding the intensity of the two directions of polarization. Figure 2 is constructed for $\lambda = 580$ nm, but for other wavelengths the intensity distribution of the rainbow is almost the same, provided that C remains fixed at the same value. However, one has to realize that C is in reality strongly wavelength dependent at any solar elevation [see Eqs. (13) and (14)].

Figure 3 shows for comparison the intensity distribution for the top ($C = 13°$) and for the base at low h ($C = 0°$) of the primary rainbow for the same Marshall–Palmer distribution and the same wavelength. However, since for the primary rainbow C is virtually independent of wavelength, there is not much wavelength dependence left for these curves. Moreover, as the result is scarcely affected by a change of C from 13° to 10°, the curve for the primary rainbow top represents a fair representation for any solar elevation.

The following features can be seen from Figs. 2 and 3:

- The intensity of the main peak of the secondary rainbow shows little difference if C ranges from 0° to 1°. For the primary bow, the large value of C at its top causes a difference in intensity[14] of the main peak of a factor of 4 with respect to the base in this simulation. For both rainbows a positive value of C shifts their main peak to a somewhat larger deviation angle.
- If $C = 1°$ is realized, the first supernumerary of the secondary rainbow is visible in the intensity distribution diagram, although its intensity is still low with respect to the main secondary rainbow maximum (certainly compared with the situation at the primary bow, Fig. 3).

To gain some quantitative insight into the possibility of observing a natural supernumerary of the secondary rainbow, we determined from the integrated rainbow intensity distributions the visibility parameter Vis of the first supernumerary as a function of C. Here, Vis is defined by

$$Vis = \frac{I_{sup} - I_{min}}{I_{sup} + I_{min}}, \tag{19}$$

where I_{min} is the intensity at the first minimum in the intensity distribution and I_{sup} the intensity of the first supernumerary, appearing at $\theta - \theta_r = 1.5°$ and 2.0°, respectively, in

Table 1. Relationship between the Quantity C, Which Determines the Strength of the Dependence of the Rainbow Angle on Drop Distortion, and the Visibility Parameter Vis of the First Supernumerary of the Secondary Rainbow

C	Vis[a]
<0.3°	0
0.50°	0.06
0.75°	0.12
1.00°	0.15
1.25°	0.17

[a] Defined by Eq. (19).

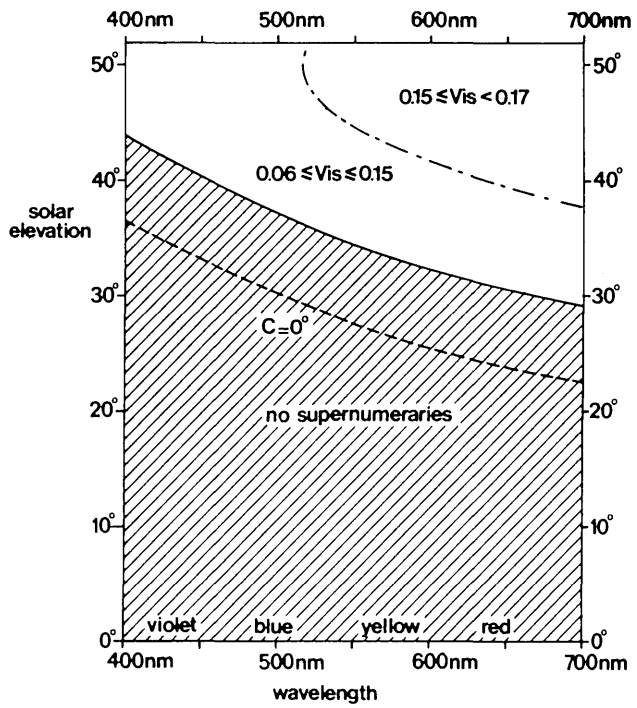

Fig. 4. Visibility diagram for the first supernumerary of the secondary rainbow in showers. If $Vis < 0.06$, supernumerary formation is impossible or highly unlikely; if $Vis \geq 0.06$, there is a chance for such formation. $Vis = 0.15$ corresponds to the situation in Fig. 2 for $C = 1°$. The line for $C = 0°$ represents the situation at which the rainbow intensity distribution is independent of flattening of drops. The most favorable conditions for supernumerary formation occur at high solar elevations and long wavelengths. If the solar elevation exceeds 51°, the rainbow top is below the horizon.

Fig. 2. The background intensity caused by externally reflected light at the drop, which is 18% of I_{sup} at $C = 1°$, is taken into account. The results, given in Table 1, show that *Vis* starts at zero for $C = 0.3°$ and increases rapidly at first. When C is of the order of 1°, *Vis* has reached 0.15 and no longer shows much variation. For the primary rainbow of Fig. 3, *Vis* = 0.18. From a comparison of these numbers we conclude that values of C of the order of 1° are still capable of creating a perceptible first supernumerary of the secondary rainbow, provided that there is not too much background intensity present from causes other than external reflected light. If *Vis* has dropped to 0.05 or below, we can consider perceptible supernumerary formation to be unlikely.

As noted before, C of the secondary rainbow is positive only if the Sun is far enough from the horizon and is strongly dependent on wavelength as well as on solar elevation. Hence, the same holds for the visibility parameter *Vis* of the supernumerary.

Figure 4 is a visibility diagram of the first supernumerary of the secondary rainbow. In this diagram a few lines of constant *Vis* have been calculated as a function of wavelength and solar elevation for the rainbow top by using Table 1 and Eqs. (13) and (14). The conclusions on the appearance of supernumeraries are the following:

- At low solar elevations, no supernumeraries of the secondary rainbow should ever be observed in showers.
- At high solar elevations, the first supernumerary may be observed, especially at the red end of the visible spectrum.
- In white light such a red supernumerary will be easily obscured by the contribution of shorter wavelengths to the rainbow, which may easily produce their main peak (see Fig. 2) at the scattering angle where this red supernumerary is supposed to appear.
- With aid of a filter, the red first supernumerary of the secondary bow may become visible in nature if the solar elevation is high enough (say, >35°).

As far as I know, no reliable observations of supernumeraries of the secondary rainbow in natural showers have been made. But in artificially made sprays, two photographs of such a supernumerary are available. The first one was taken by Greenler[15] in the infrared at $\lambda = 870$ nm at a solar elevation of about 20°; the second one is a color slide taken by Livingston at a solar elevation of about 35°. A black-and-white print of this slide taken through a red filter is reproduced as Fig. 5. Filtering improved the visibility of the supernumerary of the secondary bow significantly. The same holds for Greenler's picture: his supernumerary is weaker and apparently visible only because shorter wavelengths have been filtered. This is consistent with the last two conclusions in the preceding paragraph. But the main part of the conclusions cannot be tested with these pictures, since the drops and the drop-size distributions may differ greatly between artificially made sprays and natural show-

Fig. 5. Supernumerary of the secondary rainbow in an artificially made water spray, apparently consisting of a rather monodisperse drop-size distribution. To bring out the supernumerary, the Ektachrome original has been copied in black and white through a red filter. This procedure improves the visibility of the feature significantly. In the original, parts of the second supernumerary of the secondary rainbow are discernible too. (Photography by W. C. Livingston.)

ers. Apparently, in these pictures the supernumerary arises simply because of the presence of a favorable, rather monodisperse drop-size distribution with relatively small sizes, and the effect of flattening plays a negligible role in these cases. This can be inferred from three features in the pictures. First, the main peak of the primary rainbow in Livingston's color picture is relatively broad, and its color distribution (pale in the center[16]) indicates a predominant contribution of small drop sizes. Second, the supernumeraries of the primary bow in this picture extend to a scattering azimuth of more than 100° with a more-or-less uniform intensity, while a broad drop-size distribution would generate these supernumeraries only up to a scattering azimuth of about 70° [see Eq. (4)]. Last, for Greenler's picture the solar elevation is so low that according to our diagram no supernumerary of the secondary rainbow is to be expected in broad drop-size distributions at all, but it still shows up. Apparently, the possible generation of supernumeraries of the secondary rainbow by the ellipticity effect in broad drop-size distributions cannot be studied well in this kind of spray but should be investigated in natural showers instead.

6. CONCLUSIONS AND OBSERVATIONAL IMPLICATIONS

The existence of supernumeraries of the secondary rainbow in showers has been investigated by calculating the effect of drop distortion on the secondary rainbow angle. It was found that the dependence of this angle on the flattening of drops is much smaller than for the primary rainbow. At low solar elevations, an increase in oblateness shifts the secondary rainbow pattern toward a smaller deviation angle, which is the wrong direction for producing supernumeraries, but at high solar elevations supernumerary formation seems to be possible, especially at long wavelengths. But even then, the supernumeraries may be easily lost in the background produced by the contribution of shorter wavelengths to the light of the rainbow. These facts explain why reliable observations of such supernumeraries do not seem to exist. On the other hand, for a solar elevation larger than about 35°, it is still possible that the red first supernumerary of the secondary rainbow may be observed in nature if a monochromatic filter is used to remove the obscuring background. Obviously the chance for this is greatest in a shower displaying well-defined supernumeraries of the primary bow, but at the solar heights mentioned this primary bow can be entirely below the horizon and hence unobservable. Moreover, rainbows are infrequently seen at high solar elevations, while a sole secondary rainbow close to the horizon may easily be missed. This is also consistent with the fact that its supernumeraries are never reported. Nevertheless, a systematic investigation of secondary rainbows at high solar elevations with the aid of a red filter still has to be done and is an obvious observational next step.

The weak aspect-ratio dependence of the secondary rainbow angle may also have implications for the possibility of the formation of the hyperbolic umbilic diffraction catastrophe in highly flattened drops. An extension of the experiments of Marston and Trinh[10] to the secondary rainbow and to drops with other indices of refraction than that of water would therefore be interesting.

To summarize, the main result of the present analysis is twofold. First, it provides an explanation for the well-known fact in meteorological optics that verifiable observations of supernumeraries of secondary rainbows in showers are lacking. Second, it indicates that for high solar elevations the formation of a perceptible red supernumerary is possible in natural showers. The latter result needs observational confirmation. Greenler's[15] and Livingston's (Fig. 5) pictures cannot be considered such a proof, although their existence is interesting. Examination of natural secondary rainbows at high solar elevations with the aid of a red filter is therefore required. As the rainbow is strongly polarized,[16] its visibility and therefore the chance of detecting its red supernumerary can be improved by using the red filter in combination with a polarizing filter. Within the tradition[2,15] of observational meteorological optics it is interesting that nothing more than some simple equipment is needed to explore the existence of the red supernumerary of the secondary rainbow in open air.

ACKNOWLEDGMENTS

I thank A. B. Fraser and Th. L. van Stijn for calculations, W. C. Livingston for providing Fig. 5, and an anonymous referee for comments.

REFERENCES

1. A. B. Fraser, "Why can the supernumerary bows be seen in a rain shower?" J. Opt. Soc. Am. **73**, 1626–1629 (1983).
2. M. Minnaert, *The Nature of Light and Colour in the Open Air* (Dover, New York, 1954).
3. W. Möbius, "Zur Theorie des Regenboges und ihren experimentellen Prüfung," Abh. Kgl. Saechs. Ges. Wiss. Math.-Phys. Kl. **30**, 108–254 (1907).
4. W. Möbius, "Zur Theorie des Regenboges und ihren experimentellen Prüfung," Ann. Phys. **33**, 1493–1558 (1910). (This shortened version of Ref. 3 does not contain the derivation of this formula.)
5. F. Volz, "Der Regenbogen," in *Handbuch der Geophysik VIII*, F. Linke and F. Möller, eds. (Bornträger, Berlin, 1961), pp. 977–982.
6. H. R. Pruppacher and R. L. Pitter, "A semi-empirical determination of the shape of cloud and rain drops," J. Atmos. Sci. **28**, 86–94 (1971).
7. H. R. Prupacher and J. D. Klett, *Microphysics of Clouds and Precipitation* (Reidel, Dordrecht, The Netherlands, 1978).
8. A. W. Green, "An approximation for the shapes of large raindrops," J. Appl. Meteorol. **14**, 1578–1583 (1975).
9. P. L. Marston, "Rainbow phenomena and the detection of nonsphericity in drops," Appl. Opt. **19**, 680–685 (1980).
10. P. L. Marston and E. H. Trinh, "Hyperbolic umbilic diffraction catastrophe and rainbow scattering from spheroidal drops," Nature **312**, 529–531 (1984).
11. G. P. Können and J. H. de Boer, "Polarized rainbow," Appl. Opt. **18**, 1961–1965 (1979).
12. H. C. van de Hulst, *Light Scattering by Small Particles* (Wiley, New York, 1957), pp. 205, 245–246.
13. A. P. M. Baede, "Charge transfer between neutrals at hyperthermal energies," in *Molecular Scattering: Physical and Chemical Applications*, Vol. XXX of Advances in Chemical Physics, K. P. Lawley, ed. (Wiley, New York, 1975), p. 474.
14. A. B. Fraser, "Inhomogeneities in the color and intensity of the rainbow," J. Atmos. Sci. **29**, 211–212 (1972).
15. R. G. Greenler, *Rainbows, Halos and Glories* (Cambridge U. Press, Cambridge, 1980), Fig. 1–13, p. 19.
16. G. P. Können, *Polarized Light in Nature* (Cambridge U. Press, Cambridge, 1985), Plate 29, p. 55.